The nicotinic acetylcholine receptor and its pentameric homologues: towards an allosteric mechanism of signal transduction at the atomic level

Marco Cecchini, Pierre-Jean Corringer, Jean-Pierre Changeux

The nicotinic acetylcholine receptor and its pentameric homologues: towards an allosteric mechanism of signal transduction at the atomic level

Marco Cecchini[1], Pierre-Jean Corringer[2], and Jean-Pierre Changeux[3]

[1]Institut de Chimie de Strasbourg, UMR7177, CNRS, Université de Strasbourg, F-67083 Strasbourg Cedex, France.
[2] Institut Pasteur, Université Paris Cité, CNRS UMR 3571, Channel-Receptors Unit, Paris, France.
[3] Institut Pasteur, Université Paris Cité, CNRS UMR 3571, Department Neuroscience, Paris, France

Abstract

The nicotinic acetylcholine receptor has served, since its biochemical identification in the 1970's, as a model of allosteric ligand-gated ion channel mediating signal transition at the synapse. In recent years, the application of X-ray crystallography and high-resolution cryo-electron microscopy together with molecular dynamic simulations to nicotinic receptors and homologs have opened a new era in the understanding of channel gating by the neurotransmitter. They reveal, at atomic resolution, the diversity and flexibility of the multiple ligand-binding sites including recently discovered allosteric modulatory sites distinct from the neurotransmitter orthosteric site and the conformational dynamics of the activation process as a molecular switch linking together these multiple sites. The model emerging from these studies paves the way to a new pharmacology based, first, upon the occurrence of an original mode of indirect allosteric modulation, distinct from a steric competition for a single and rigid binding site and, second, the design of drugs specifically interacting with privileged conformations of the receptor such as agonists, antagonists and desensitizers. The research on nicotinic receptor is still at the forefront in understanding the mode of action of drugs on the nervous system.

Introduction

Louis Pasteur (1886) already recognized that the action of certain substances on the nervous system is mediated by defined components of the living matter and stated about the difference in taste of isomeric forms of sugars, that a "dissymmetric active body would play a role in the nervous impression". This view was further elaborated by Paul Ehrlich (1885) and most of all by John Newport Langley (1905) who sought to localize and specify the target of curare and nicotine in neuromuscular preparations and concluded that "the muscle substance which combines with nicotine and curare is not identical with the substance which contracts... I have called it the *receptive substance* or today's "receptor".

It took almost 65 years to identify the first receptor for a neurotransmitter: the nicotinic acetylcholine receptor (nAChR) (1) ; rev in (2). This was made possible by the joint use of the electric organ of fish as a rich source of receptor and α-bungarotoxin (α-Bgtx), a snake venom toxin with exquisite specificity (3); rev in (2). Subsequent reconstitution studies showed that nAChR is an integral membrane protein of molecular mass about 290 kDa that possesses all the structural elements

necessary to mediate the electric response to a synaptic pulse of ca $3x10^{-4}$ M ACh in the millisecond timescales (motor endplate).

1. The nAChRs: an unconventional allosteric protein

Patch-clamp techniques revealed that the electric response represents a population of single openings of a square shape with risetime in the microsecond range and mean open duration of a few milliseconds. In addition, prolonged application of ACh or nicotine was found to block subsequent receptor responses, a process termed desensitization which was assumed to slowly (on a 100 ms to s timescale) stabilize a new high-affinity closed (refractory) state of the receptor referred to as desensitized (4–6).

An important step was the demonstration that these electrical phenomena have a structural basis. First data unambiguously showed that in the native membrane the receptor is present in a state which binds cholinergic agonists with low affinity; prolonged exposure to the agonist then stabilizes the receptor in a slow (seconds, minutes) and reversible manner, in a high affinity state for agonists. Then, time-resolved rapid mixing techniques were developed with fluorescent agonists like dansyl-C6·choline (7) or isotopically labeled cholinergic ligands and rapid filtration (8), and changes in intrinsic or extrinsic fluorescence after labelling of the receptor with fluorescent probes (9, 10) and Refs. in (11). Studies with dansyl-C6·choline and [^{3}H]-ACh showed that in addition to the slow desensitization on the second time scale, a faster conformational transition to an *intermediate state* called I (12) would occur with a rate constant of 2 s^{-1} (13) to 50 s^{-1} (14). Parallel functional studies using the same membrane preparation revealed that the I transition fits with a fast desensitization of the response (12). A simple 4-state model was found compatible with the concerted model for allosteric transitions (15) and that proposed by Katz and Thesleff (16) for desensitization; rev in (17).

To sum up, the *in vivo* and *in vitro* data demonstrate that the receptor protein interconverts between – at least – four discrete conformations: (i) a resting closed-channel state (R) stabilized by nicotinic antagonists; (ii) an active, fast, open-channel state (A) with low affinity for ACh and nicotinic agonists; and (iii) fast (I) and slow (D) desensitized states with higher affinities for ACh and nicotinic agonists (but also for some antagonists). Contrary to an opinion widespread among pharmacologists, the highest-affinity states do not correspond to the active state of the receptor—far from it. On the other hand, the relatively low affinity of the active state permits fast and repetitive transmission (18, 19).

2. Functional architecture of nAChRs

Early biochemical dissection of the isolated nAChR from *Torpedo* electric organ revealed that it spontaneously forms oligomers comprising five homologous subunits with the arrangement of α1-γ-α1-δ-β. They are symmetrically arranged around a central ion channel, with a five-fold symmetry axis perpendicular to the membrane. The primary structure of each subunit established through protein sequencing and cDNA cloning and sequencing revealed a large hydrophilic amino-terminal extracellular domain (ECD), a transmembrane domain (TMD) comprising four hydrophobic segments (M1–M4), and a variable hydrophilic intracellular domain (ICD). The ECD harbors two ACh binding sites at the α1-δ ad and α1-γ interfaces, that are functionally linked to the centrally located cationic channel in the TMD almost 60 Å away (rev (17, 19)). The gating of the ion channel by ACh that takes place between topographically far distant sites is an unquestionable allosteric interaction. Moreover, the different conformations of the receptor including the active state have been observed even in the absence of ACh (20), validating the fundamental premise of the Monod-Wyman-Changeux (MWC) model (15) and ruling out an exclusive induced-fit mechanism. The nAChR protein thus possesses all the structural elements required to convert a chemical signal into an electrical response and mediates the inter-cellular communication between neurons acting as an 'allosteric switch' (21).

17 genes code for nAChR subunits in the human genome leading to an astronomic number of possible oligomeric combinations in pharmacologically distinct hetero- and homo-pentamers. However, the most represented compositions *in vivo* include the muscle-type α1βγδ nAChR, the neuronal α4β2 and α3β4 nAChRs, and the homopentameric α7 nAChRs. nAChRs belong to the superfamily of pentameric ligand-gated ion channels (pLGICs) present in bacteria and animals, which also comprises the major mammalian neurotransmitter receptors for serotonin ($5HT_3R$), glycine (GlyR), and γ-aminobutyric acid ($GABA_AR$). nAChRs and $5HT_3Rs$ form a subfamily mediating excitatory transmission, carrying an ion channel selective of Na^+, K^+ and sometimes Ca^{2+}, whereas GlyRs and $GABA_ARs$ are inhibitory receptors with an anion (Cl^-) selective channel (19).

2.1 The orthosteric site and the ion channel

Before the advent of high-resolution (3D) structures of nAChRs in 2000, the principal functional sites of the receptor had been explored by affinity labelling and mutagenesis approaches. These experiments showed that the neurotransmitter or orthosteric binding site is in the EC domain at the interface between subunits. Three regions from the ''principal'' subunit (loops A, B, and C) and four from the ''complementary'' subunit (loops D, E, F, and G) contribute to the binding pocket (22). Loops A (Tyr), B (Trp), C (two Tyr), and D (Trp) form an aromatic box or cage chelating the ammonium group of ACh with the tryptophan residue from loop B establishing a direct cation-π interaction (23).

The ion channel function was initially explored with blockers that bind within the TM domain and prevent ion fluxes by sterically occluding the channel pore (rev in (17, 24)). Early affinity-labeling experiments with channel blockers such as chlorpromazine (25, 26) or trimethyl phenyl phosphonium (TPMP) (27) identified key residues within the segment M2 at positions 2′, 6′, 9′, 13′ and 20′ for each subunit of the pentamer; i.e. the conventional prime numbering starts at zero after the universally conserved positively charged residue at the cytoplasmic end of the pore (rev in (28)). This showed that the same side of each M2 helix 'faces' the ion pore and that the walls of the channel consist of pentameric rings of homologous amino acids. Three rings of negatively charged residues frame the amino acid clusters labeled by chlorpromazine and were found by single channel recording to contribute to cation permeation (29, 30). Later on, using site-directed mutagenesis the region comprising M2 and the short loop bridging M1 and M2 was identified as the one governing the selectivity of the channel for cations in nAChRs and anions in GlyRs (31). This allowed to locate the selectivity filter of nAChRs at the cytoplasmic entrance of the pore, where a ring of glutamates at position −1′ directly interacts with and selects for cations, while repelling anions.

2.2 The allosteric modulatory sites

An important outcome of the research on the allosteric properties of nAChRs (and pLGIC more generally) has been the discovery of diverse categories of modulatory sites, with positive or negative effects on the signal transduction mechanism. These modulatory sites are referred to as 'allosteric' in the sense that they are topographically distinct from the orthosteric site and modulate channel gating indirectly. Benzodiazepines, the currently most prescribed psychoactive drugs, were the first allosteric modulator of pLGICs ever described. They allosterically modulate $GABA_A$ receptors (32, 33) at sites located in the synaptic extracellular domain (34, 35). Ca^{2+} ions were the first positive allosteric modulator recognized with nAChRs (36, 37). They bind to a region distinct from the ion channel (section III) near the interface between the EC and TM domains (38, 39). Several hydrophobic molecules that bind to the TMD were found to display robust allosteric effects. First, the TM domain is embedded in the lipid bilayer, and specific lipids including cholesterol and anionic lipids are required for proper function of the Torpedo nAChR. However, it is not clear at present if lipids alter the structure and function of nAChRs though binding to allosteric sites, or by altering bulk membrane physical properties; for recent reviews on nAChR-lipids interaction, see (40) and (41). Small amphipathic molecules including short-chain alcohols and general anesthetics typically inhibit nAChRs and potentiate the inhibitory GlyRs and $GABA_A$Rs, both contributing to anesthesia (42). The anthelmintic ivermectin (IVM), first discovered by Omura and Campbell (43), is a

PAM at α7-nAChR (44) but also a PAM at the worm inhibitory receptor GluCl, where it enhances muscle inhibition and promotes worm paralysis, and GlyR (45). PAMs of nAChRs include a variety of natural and synthetic compounds (46) that have been subdivided in two groups. Those that increase the acetylcholine (and nicotinic agonists) activation peak current with little or no effect on desensitization are referred to as *type-I*. Those that delay and slow down the desensitization kinetics and, in some cases, even reactivate previously desensitized receptors are referred to as *type-II* (47). Ivermectin (48) and 5-hydroxyindole (49) are typical type-I PAMs at α7 nAChRs, whereas synthetic compounds like PNU-120596 (50) or TQS (51) are type-II. These compounds can act directly by binding to allosteric sites, by indirectly displacing already bound lipids, or both. Positive and negative modulators of nAChRs have been recently curated in a database named ACRALL (52).

Finally, nAChRs are also allosterically modulated by intracellular factors. The ICD carries several phosphorylation sites that modulate desensitization (53). For the muscle-type nAChR, the ICD tightly binds to rapsyn, a scaffolding protein that contributes to targeting and aggregation of receptors at the neuro-muscular junction (54, 55). Growing evidence also suggests that α7-nAChR binds to G proteins and may even mediate an agonist-elicited metabotropic function through stabilization of the desensitized state (56, 57).

3. High-resolution structures

3.1 Overall molecular architecture

Early structural data on the nAChR protein were obtained by processing electron microscopy (EM) images of purified proteins from *Electrophorus electricus* and AChR-rich membranes from *Torpedo marmorata* (58–60). The images revealed ring-like particles (8–9 nm in diameter) with a hydrophilic central core (about 1.5 nm) surrounded by a compact bundle made up of several (approximately five) subunits. Following the discovery that AChRs may form closely packed two-dimensional assemblies in *Torpedo marmorata* postsynaptic membranes (Brisson 1980 PhD thesis), substantial enhancement of map quality up to 4 Å was achieved (61, 62), yet without reaching atomic resolution. First *bona fide* models of the ACh-binding domain and binding site came from crystallographic studies of the acetylcholine binding protein (AChBP) (63), a water-soluble homolog of nAChR devoid of the TMD that is naturally occurring in some invertebrates, yet without the conformational changes mediating receptor's activation.

For decades nAChRs from the fish electric organ resisted to crystallization. The discovery of prokaryotic homologs in bacteria (64, 65) revealed an unanticipated subfamily with a wide range of

functional properties that were amenable to X-ray crystallography. The GABA-gated ELIC was first solved in a closed-channel conformation (66). The proton-gated GLIC was then solved in both closed- and open-channel conformations (67–69), providing the first insights onto the conformational changes mediating signal transduction. Recently, other bacterial pLGICs were solved, including the high-pH-gated STELIC (70) and DeCLIC the first pentameric channel naturally fused to a periplasmic domain (71).

Riding the wave of success in bacteria, eukaryotic pLGICs were finally solved by X-ray crystallography starting with the GluCl receptor from invertebrates (72) followed in chronological order by GlyR (73), $GABA_AR$ (74), $5HT_3R$ (75), and the first nAChR (76). Most recently and thanks to several improvements in cryo-EM detectors and *ad hoc* measures to enhance protein expression, biochemical stability, and particles alignment, several high-resolution structures of nAChRs have been deposited (77). At the time of this review, 27 high-resolution structures of integral membrane nAChRs are available in the PDB; see **Table I**. They include the muscle-type α1βγδ and the homomeric α7 nAChRs in multiple states, and the neuronal heteromeric α3β4 and α4β2 nAChRs in a single state.

Overall, the structural data collected so far point to a striking conservation of the molecular architecture of pLGICs from bacteria to mammals. The 3D structures illuminate both symmetrical and pseudo-symmetrical organizations made of five identical or homologous subunits. Each subunit is modular and consists of a 190–200 amino acids ECD organized in a β-sandwich including inner and outer β-sheets, and a TMD composed of four α-helices (M1–M4). In agreement with biochemical studies (section I) the M2 α-helices line the ion pore and interact with M1 and M3, which in turn interact with M4 located at the periphery of the protein and most exposed to lipids. In the eukaryotic receptors a third intracellular domain (IC) made of two α-helices (MX and MA) provides a platform for intracellular regulation; see **Figure 1**.

Table 1. High-resolution structure of nAChRs deposited in the PDB.

Type	ligand	other ligand(s)	modulator(s)	state	PDB	organism	Res. [A]	Publication
αβγδ	apo	lipids	-	R	7QKO	*Tetronarce californica*	2,9	Zarkadas_2022
αβγδ	carbamylcholine		agonist	D	7QL6	*Tetronarce californica*	3,2	Zarkadas_2022
αβγδ	d-tubocurarine	d-tubocurarine	antagonist	D	7SMS	*Tetronarce californica*	3,18	Rahman_2022
αβγδ	carbamylcholine		agonist	D	7SMR	*Tetronarce californica*	2,83	Rahman_2022
αβγδ	carbamylcholine	d-tubocurarine	agonist/anta	D	7SMT	*Tetronarce californica*	2,61	Rahman_2022
αβγδ	α -bungarotoxin	lipids	antagonist	R	6UWZ	*Tetronarce californica*	2,69	Rahman_2020
αβγδ	nicotine		agonist	D	7QL5	*Tetronarce californica*	2,5	Zarkadas_2022
αβγδ	apo		-	R	7SMM	*Tetronarce californica*	2,57	Rahman_2022
αβγδ	apo	cholesterol	??	R	7SMQ	*Tetronarce californica*	2,82	Rahman_2022
αβγδ	α-short-neurotoxin (ScNTx)		antagonist	R	7Z14	*Tetronarce californica*	3,15	Nys_2022
αβγδ	rocuronium	cholesterol	antagonist	R	8ESK	*Tetronarce californica*	2,90	Goswami_2023
αβγδ	rocuronium (pore-blocked)	cholesterol	antagonist	R	8F2S	*Tetronarce californica*	2,90	Goswami_2023
αβγδ	choline	etomidate	agonist/NAM	D	8F6Y	*Tetronarce californica*	2,79	Goswami_2023
αβγδ	succinylcholine		antagonist	D	8F6Z	*Tetronarce californica*	2,70	Goswami_2023
α7	EVP-6124		agonist	D	7EKP	*Homo sapiens*	2,85	Zhao_2021
α7	apo	cholesterol	-	R	7EKI	*Homo sapiens*	3,18	Zhao_2021
α7	EVP-6124	PNU-120596	agonist/PAM	D-open	7EKT	*Homo sapiens*	3,02	Zhao_2021
α7	epibatidine	calcium ions	agonist	D	7KOQ	*Homo sapiens/E. coli*	3,6	Noviello_2021
α7	epibatidine	calcium ions, PNU-120596 (?)	agonist/PAM	A	7KOX	*Homo sapiens/E. coli*	2,7	Noviello_2021
α7	α -bungarotoxin	calcium ions	antagonist	R	7KOO	*Homo sapiens/E. coli*	3	Noviello_2021
α7 (ECD)	apo	C4	-	R	8C9X	*Homo sapiens*	2,46	Prevost_2023
α7 (ECD)	nicotine	C4	agonist/PAM	A/D-like	8CAU	*Homo sapiens*	3,51	Prevost_2023
α7 (ECD)	apo	C4	-		8CI2	*Homo sapiens*	3,4	Prevost_2023
α7 (ECD)	apo	E3	ago-PAM	A/D-like	8CE4	*Homo sapiens*	2,53	Prevost_2023
α7 (ECD)	nicotine	E3	agonist/PAM	A/D-like	8CI1	*Homo sapiens*	2,7	Prevost_2023
α7 (TMD+ICD)	apo		-	R	7RPM	*Homo sapiens*	NMR	Bondarenko_2022
α7 (TMD+ICD)	ivermectin		agonist	D	8F4V	*Homo sapiens*	NMR	Bondarenko_2023
α4β2	varenicline	N.D.	agonist	D	6UR8	*Homo sapiens*	3,71	Mukherjee_2020
α4β2	varenicline + BAK5	N.D.	agonist	D	6USF	*Homo sapiens*	3,87	Mukherjee_2020
α4β2 (2α:3β)	nicotine	cholesteryl-hemisuccinate	agonist	D	6CNJ	*Homo sapiens*	3,7	Walsh_2018
α4β2 (3α:2β)	nicotine	cholesteryl-hemisuccinate	agonist	D	6CNK	*Homo sapiens*	3,9	Walsh_2018
α4β2	nicotine	N.D.	agonist	D	5KXI	*Homo sapiens*	3,94	Morales_2016
α3β4	AT-1001		partial agonist	D	6PV8	*Homo sapiens*	3,87	Gharpure_2019
α3β4	nicotine		agonist	D	6PV7	*Homo sapiens*	3,34	Gharpure_2019

3.2 Ligand binding sites and conformational transitions at atomic resolution

High-resolution structures of nAChRs provide a detailed 3D description of the binding pockets of key classes of effectors as well as the conformational transitions they promote. In the following, we present the details of the orthosteric site, the ion transmitter pore, and the allosteric binding sites emerging from the currently available structures.

The orthosteric site. Agonist-bound structures solved in complex with carbamylcholine, the natural alkaloids nicotine and epibatidine, and synthetic ligands like varenicline, EVP-6124 and AT-1001 illuminate the details of agonist binding. In agreement with the biochemical data (section I), the agonist-binding site lies at the interface between subunit in the ECD. All agonists bear a key electropositive ammonium moiety that is stabilized by hydrogen-bonding and characteristics cation-π interactions with the cage of five aromatic residues first identified by affinity labeling (78–80); rev in (11). A second key pharmacophore is a H-bond acceptor that interacts directly or via a bridging water (81) with a main chain H-bond donor from loop E of the complementary subunit. Last, high-resolution structures of the heteromeric α4β2 and α3β4 nAChRs show that the guanidinium group of an arginine from loop B at both β2 and β4 subunits engages in cation-π interactions with two tyrosines of the aromatic cage thus occupying the ammonium binding site. This observation highlights that orthosteric sites of heteromeric receptors are not equivalent and rationalizes why orthosteric ligands bind to the α-β interface and not to β-α or β-β interfaces in α3β4 and α4β2 nAChRs.

Competitive antagonist-bound structures including snake toxins (82–84), the active component of curare (85), and synthetic neuromuscular blockers (86) illuminate the details of the orthosteric site in the inhibited state(s) of the receptor. Compared to the agonist-bound state, most structures display a less compact ECD with a C-loop stabilized in a splayed-open conformation like the one found in the absence of ligands (*apo*) (85, 87, 88). With rocuronium, the additional volume is occupied by the ligand that is larger and bulkier than any known agonist. In the α-toxin-bound structures, this volume is occupied by finger II of the toxin that inserts and penetrates deeply in the orthosteric pocket. An arginine and a phenylalanine with α-Bgtx or a histidine with α-short-chain neurotoxin (ScNtx) stack in a cation-π sandwich with the highly conserved tyrosine from loop C (82–84). Altogether, these structures suggest that bulky competitive antagonists stabilize an inhibited conformation of the receptors by preventing C-loop capping at the orthosteric site along with the compaction of the ECD. In sharp contrast, structures solved with depolarizing muscle blockers like succinylcholine (86) or *d*-tubocurarine (85), feature a fully closed or semi-closed C-loop in a configuration resembling that found with

agonists. Consistent with functional experiments showing that large antagonists stabilize the resting state (89) whereas smaller antagonists enhance desensitization (90), the structural data suggest that substances like curare and depolarizing muscle blockers may promote receptor inhibition by acting as desensitizers.

The ion transmitter pore. The "active site" of nAChRs is arguably the ion transmembrane pore that opens and closes in response to agonist binding. In agreement with early biochemical data (section I), high-resolution structures of nAChRs demonstrate that the ion transmembrane pore is formed by the M2 helices at the pentameric axis of symmetry. Based on the pore configuration, the available structures can be roughly divided into two groups: i. those with no ligand (*apo*) or with large antagonists bound at the orthosteric site feature a straight orientation of the M2 helices that produces a hydrophobic constriction in the mid of the membrane at positions 9′, 13′ and 16′; and ii. those with agonist bound that feature tilted M2 helices with a constriction point near the cytosol formed by five glutamates at position −1. The permeability of these conformations to both ions and water has been tentatively assigned based on static measurements of the pore diameter using tools like the software HOLE (91) or CHAP (92) (see below 4.1). Since both classes feature a minimum pore diameter that is smaller than that of partially hydrated cations (e.g., Na^+), all structures were annotated as non-conductive. In addition, the strong hydrophobic character at the constriction point of the apo-like structures appears inconsistent with the translocation of ions and possibly water and these structures can be reasonably assigned to the resting state. Such "hydrophobic gating" (93) in the middle of the pore has been consistently observed in all pLGICs. By contrast, in the agonist-bound structures the constriction is formed by a ring of negatively charged residues on the cytosolic side of the TMD, whose side chains can plausibly adapt to a cation allowing for chelation and translocation. The cryo-EM densities of α4β2 and α3β4 bound to nicotine indicate that these glutamates at position −1′ likely coordinate a monovalent cation, which was proposed to prevent cation permeation by electrostatic repulsion (81). Thus, all agonist-bound structures together with those in complex with small antagonists like succinylcholine or d-tubocurarine were annotated as desensitized. Consistent with this conclusion, anionic pLGICs with agonist bound feature a similar conformation of the ion pore with a hydrophobic constriction near the cytosol (94). However, one cannot rule out the hypothesis that the desensitization gate is located differently at nAChRs, e.g., at position 9' as suggested by recent simulations of α7-nAChR (95), and that the surprising organization of five glutamates at bottom of the TMD is physiologically irrelevant.

Finally, two structures of the α7-nAChR recently solved by cryo-EM in the presence of agonist and a large excess of PNU-120596 (PNU) (84, 87) illuminated a distinct organization of the ion channel. Interestingly, the cryo-EM densities indicate that PNU binding causes significant widening of the ion pore in the mid of the TMD, mostly due to the rearrangement of the L9' side chains that rotate out of pore axis. Since PNU is a type-II PAM of α7 that is able to reactivate previously desensitized receptors [Park2009], these structures were tentatively assigned to the activated state of the receptor (84) and a partially desensitized or partially open state (87), respectively. Albeit suggestive and reminiscent of the cryo-EM of $5HT_3R$ solved under activating conditions (96), the relevance of these receptor conformations remains unclear. In particular, the structure of the supposedly active state of α7-nAChR shows a significant compression (by 5-10 Å) of the TMD in the direction perpendicular to the membrane, which is not observed in the R state (before activation) or the D state (after activation). Such a compression results in significant tilting of the TM helices along with vertical sliding of the helix M4, which produces partial helical unwinding at the M4-MA junction. These energetically costly rearrangements were proposed to mediate ion permeation via the widening of the lateral fenestrations in the ICD (84). However, recent simulation analyses have shown that ions may freely diffuse to the intracellular vestibule through these portals even in structures with intact M4-MA junctions (95). Given the peculiarity of the PNU-bound structures, more studies are needed to assess their physiological significance.

In the limit of functional annotations based on static structures, the data collected at nAChR indicate that in the R state, the ion channel is shut by a patch of bulky hydrophobic residues in the mid of M2 (activation gate), whereas the location of the desensitization gate remains debated.

The intracellular domain. The ICD plays a critical role in pentameric assembly, trafficking, sub-cellular localization, allosteric signaling and channel conductance (19, 97). Following the seminal work of Gharpure *et al* on α3β4 (81), several high-resolution structures of the ICD in nAChRs have been obtained. The structural data indicate that each subunit contributes to the ICD with a short post-M3 loop, a short amphipathic MX helix that lies parallel to the membrane plane, a poorly conserved and disordered cytoplasmic loop name loop L, and a long MA helix that protrudes ~40 Å into the cytosol. These helices form a pentameric bundle that frame five lateral portals for ion permeation. These portals are lined by both acidic and polar residues that provide a favorable environment for cation permeation and charge reversal at these sites was shown to attenuate the single-channel conductance (81). Perhaps surprisingly, the MA-helical

bundle does not undergo major conformational changes in the agonist-bound versus antagonist-bound structures (85) with the lateral fenestrations being large enough (8-12 Å) to allow for the permeation of hydrated cations even in the resting state (82). Strikingly, the poorly conserved L-loop is solved in no structure of intact nAChRs. Recently, Bondarenko *et al* modelled the structure of a smaller and functional construct encompassing the TMD and ICD of the human α7-nAChR using structure restraints from NMR and ESR spectroscopy (98). This structure offered the first glimpse of the 3D architecture of the ICD including loop L, which appears to harbor three short helical segments adopting a characteristic "B-shape". The large fraction of formally charged residues (18 pairs) unevenly distributed along the sequence results in regions with a net positive charge in the upper ICD that interact with lipids from the inner leaflet, and regions with a net negative charge in the lower ICD that likely bind cytoplasmic partners.

The allosteric binding site(s). The currently available structures illuminate five allosteric sites at nAChRs with atomic resolution, in addition to several lipid-binding sites (**Figure 2**). The structure of α7-nAChR with PNU bound illuminates the details of an intersubunit allosteric site in the TMD (87). In this structure, PNU inserts deeply at the interface between subunits making interactions with M2 and M3 from the (+)-subunit and M1 and M2 from the (−)-subunit. This modulatory site is located on the extracellular side of the TMD and strongly overlaps with the ivermectin-binding site first illuminated with GluCl (72) and GlyR (73, 99). The recent NMR structure of a TMD+ICD functional construct from α7-nAChR, which is activated by IVM, provides evidence that IVM binds to the same intersubunit allosteric site as PNU, albeit more superficially (100). Since IVM is a type-I PAM of α7-nAChR (44), the structural data suggest that the depth of ligand insertion may be critical for the modulation of desensitization.

The structure of the muscle-type nAChR in complex with the antagonist d-tubocurarine (d-tubo) shows toxin density in two unexpected allosteric sites in addition to the classical orthosteric sites (85). In this structure, d-tubo binds at both the extracellular entrance of the ion pore and the periphery of the TMD at the junction between M1, M3, and M4 (**Figure 2**). Interestingly, in the latter binding mode, d-tubo appears to stabilize a "detached" conformation of the M4 helix, which moves away from the receptor core. Since a similar uncoupling of M4 was proposed to produce slower recovery from desensitization (85), both the peripheral and the pore-blocking binding sites are potential sites for negative allosteric modulation. Consistently, a similar intrasubunit site with a detached M4 was found in the cryo-EM structure of the muscle nAChR in complex with the general anesthetic etomidate (86). Of note, the numerous cryo-EM structures of the muscle nAChR show electron density allowing partially constructing lipids,

including cholesterol and phospholipids, bound at the interface between the receptor and the lipid-bilayer. However, depending on the biochemical preparation, these lipids are found at somewhat different locations and in different poses in the grooves between the TMD helices. The contribution of each lipid-binding sites to allosteric modulation remains at present unclear; see (40) for a recent review.

In the ECD, recent cryo-EM studies of α7-nAChR illuminated the details of the regulatory site for calcium (84) and revealed a novel intersubunit allosteric site at the apex of the ECD (101). In agreement with early biochemical studies, the cryo-EM structures of α7-nAChR revealed strong ball-shaped densities in proximity of the β1-β2 loop and the Cys-loop consistent with calcium binding at the ECD-TMD interface (84); see **Figure 2**. These motifs carry glutamate residues whose mutation abolishes calcium potentiation (38) and were annotated as PAM binding sites. Interestingly, homologs of the Ca^{2+}-binding sites have been characterized with bacterial channel ELIC, where divalent cations including Ba^{2+} behave as negative modulators (102). Most recently, the structure of the α7-nAChR ECD was solved in complex with two allosteric nanobodies (101) obtained through immunization of alpacas to generate highly potent and α7-specific modulators (103). This previously unrecognized allosteric site is located at the apex of the pentameric architecture lined by the long β2-β3 loop, a.k.a. MIR, and the top α-helices from both principal and complementary subunits. Interestingly, the high-resolution structures of the complex reveal a symmetric pentameric assembly of the nanobodies extending the ECD that is reminiscent of homologous receptors carrying a regulatory N-terminal domain (71); see **Figure 2**.

Altogether, the recent cryo-EM analyses of nAChRs illuminate the details of five allosteric ligand-binding sites scattered along the protein structure. Given the large size of receptor, other modulatory sites likely remain to be characterized. Currently missing sites include those identified in other pLGICs, such as benzodiazepines sites at the non-orthosteric interfaces of $GABA_A$ receptors (34, 104, 105), sites directly above the orthosteric site (106) or on the vestibular side of the orthosteric site (107), or TMD sites like the intrasubunit site for general anesthetics found in GLIC and their relationships with membrane lipids (42).

4. Mechanisms of activation and desensitization

The conformational transitions between the physiological states of the receptor involve a global reorganization of the protein that can be spontaneous or stabilized by effector binding. The characterization of these conformational changes, referred to as *allosteric transition pathways*,

with atomic resolution is challenging since it potentially involves a multitude of transient conformations. In addition, nAChRs have been fine-tuned to achieve signal transduction on the sub-millisecond timescale, as shown in fast-perfused outside-out patch clamp recordings (108), which makes them challenging to probe by direct functional assays. Last, experimental structural determinations with atomic resolution illuminate receptors in states that are often stabilized in non-physiological conditions, i.e., trapped in crystals or frozen in thin vitreous ice with the lipid membrane replaced by detergent micelles or lipid nanodiscs, and provide little dynamic information. In this context, time-resolved analyses by computer simulations and/or functional assays, e.g., with the incorporation of fluorescent probes, can go beyond structures providing mechanistic insights at physiologically relevant conditions.

4.1 Functional annotation of structures

The functional annotation of ion-channel structures from X-ray crystallography and cryo-EM is difficult albeit essential. As previously discussed, the extrapolations of channel permeability from geometric analyses of the pore are limited and cannot account for protein-buffer and protein-membrane interactions, nor the conformational dynamics of the protein. To overcome these limitations, specialized simulation approaches have been developed. Assuming that pore hydration can be used as a proxy for channel conductance, Trick *et al* proposed a functional annotation of ion-channel structures based on the analysis of the water density inside the pore (109). Alternatively, pore permeability can be probed by single-ion free energy profile calculations based on umbrella sampling (109) or enhanced sampling simulations (95). Although computationally more involved, these calculations provide information on the energetics of ion permeation and selectivity. More recently, molecular dynamics (MD) simulations with voltage applied were used to predict the channel conductance and selectivity by counting the number of ion-translocation events in finite time windows, a method called "in-silico electrophysiology" (110). In the case of GlyR, such analyses predicted that an early cryo-EM structure of a presumed active state solved in detergents (73) was fivefold more conductive for Cl^- relative to experiments and was non-selective to polyatomic anions (110). Remarkably, the relaxation of this "wide-open" state by MD simulations in a lipid bilayer yielded a narrower open-channel state that recapitulated the permeation properties by electrophysiology (110, 111) and was experimentally validated by subsequent cryo-EM studies of GlyR in a native-like lipid environment (112). Most recently, computational electrophysiology combined with single-channel recordings and site-directed mutagenesis revealed the existence of lateral fenestrations

for Cl^- translocation in the ECD of GlyR, which explain the origin of current rectification in known anomalous mutants (113).

In AChRs, MD analyses of recent high-resolution structures have started to provide additional insights. For example, the agonist-bound structures of α3β4 and αβγδ initially annotated as desensitized were found to carry a fully hydrated pore both in backbone-restrained (88) and unrestrained (81) simulations, somewhat suggesting for an ion-conductive pore. Simulation studies of α7 by all-atom MD, ion-permeation free energy profiles, and in silico electrophysiology provided evidence that the structure in complex with α-Bgtx is nonconductive, the one solved with agonist+PNU is conductive and cation-selective, and the one solved with agonist alone is nonconductive plausibly representing the desensitized state (95). Interestingly and in contrast with previous conclusions, these analyses suggest that the desensitization gate is located at the hydrophobic ring at position 9′, somewhat overlapping with the activation gate (95). Considering the gap between static structures frozen in detergents and membrane-inserted functional receptors, further simulation analyses are likely to provide more mechanistic insights in the future.

4.2 The mechanism of ion-channel activation with atomic resolution

The classical MWC interpretation of ion-channel activation or *gating* in nAChRs is based on an equilibrium model that does not aim at describing the trajectory connecting the end states of the transition. However, the mechanism underlying signal transduction involves a dynamic process between these states, whose details have been explored for more than 50 years. Computational analyses based on all-atom MD have been extensively used to break through the dynamic nature of the phenomenon and shed light onto the sequence of structural events translating neurotransmitter binding into pore opening with atomic resolution. Early studies based on homology models of α7 and short unbiased MD (114) or targeted MD (115) simulations highlighted a strong correlation between closing of C-loop at the orthosteric site and opening of the activation gate via twisting of subunits in the ECD and outward tilting of the M2 helices in the TMD. Simulation work on the X-ray structures of GLIC (116) and GluCl (117, 118) with agonist removed (i.e., un-gating) provided evidence for an indirect coupling between agonist binding and pore opening, suggesting that global receptor *twisting* elicited by agonist unbinding would “lock” the channel in a non-activatable resting state. In addition, these studies predicted that a global expansion/contraction of the ECD referred to as *blooming* was a key element of the allosteric mechanism, which was later on confirmed by the X-ray structures

of GLIC and GluCl solved in the absence of agonist (69, 119). By modeling agonist binding in the resting state of $5HT_3R$ and MD relaxation, the gating mechanism was also probed in the forward direction (120). The simulations revealed that the structural stress introduced by ligand binding at the orthosteric site could be released via contraction of the ECD (i.e., un-blooming) and repositioning of loops at the ECD-TMD interface (i.e., M2-M3, β1β2, and Cys-loop), which promote the stabilization of a water-permeable ion pore via the outward tilting of M2 and M3 and the interconnecting loop. In addition, these simulation suggested that ion permeation would require the conformational switch of two rings of hydrophobic residues at the activation gate (i.e., L9′ and V13′) to reduce steric hindrance (120). More recently, using the string method with swarms of trajectories, Lev *et al* provided a detailed model of activation in the proton-gated GLIC including a description of the energetics involved (121). In addition to account for the modulation by pH, this model of gating introduced a new element in the allosteric mechanism highlighting the role of the contraction/expansion of the extracellular β-sandwiches at the ECD-TMD interface, which was validated by fluorescence experiments (122). Only very recently, MD simulations were used to characterize the allosteric communication pathways in nAChRs (123). Using a large number of non-equilibrium MD simulations, it was shown that agonist removal from the orthosteric site of the nicotine-bound α4β2-nAChR produces an extremely fast wave of conformational rearrangements propagating from the C-loop in the ECD to the M2-M3 linker at the ECD-TMD interface on the nanosecond time scale. Although these calculations are too short to capture the large-amplitude changes underlying activation, they highlight the implication of loop F in the allosteric mechanism. Strikingly, the same communication pathway was also detected in α7-nAChR (124).

Altogether, the simulation analyses of nAChRs and homologs suggest that the transition from resting to active involves a series of discrete conformational changes that start at the level of the orthosteric site with C-loop closing and are transmitted and amplified via: (1) tilting of the extracellular subunits, which results in a global contraction or un-blooming of the ECD; (2) repositioning of loops at the ECD-TMD interface; (3) the outward displacement of the M2-M3 linker coupled to tilting of the pore-lining helices M2; and (4) opening of the activation gate via rotameric transitions of bulky and hydrophobic residues on M2 that promotes pore wetting and ion permeation. The details of such a *conformational wave* translating agonist binding to pore opening are illustrated in **Figure 3A**. In addition, simulation analyses of nAChRs and homologs indicate that the allosteric communication between the orthosteric site and the ion

pore involves a *weak coupling* mechanism[1], where nearly autonomous quaternary changes at the ECD or TMD stabilized by ligand-binding events are communicated at the ECD-TMD interface via shape complementarity rather than specific residue-residue interactions. Consistent with this idea, isolated ECD and TMD were shown to fold spontaneously when properly engineered (125, 126), and combinations of ECDs and TMDs from different receptor families often generate functional chimeras (127). This mechanism is also supported by aggressive mutagenesis studies at the ECD-TMD interface (128). A weak coupling mechanism for gating, which is reminiscent of the functioning of biomolecular motors (129) and artificial molecular nanomachines (130), naturally accounts for the occurrence of non-conducting intermediates on the way to activation, which are discussed below.

4.3 The multi-step transition pathway of activation

The MWC model was based upon discrete states in thermodynamic equilibrium and did not bring insights on the dynamic of their interconversion. The development of technologies made this accessible. Among the biophysical methods to monitor proteins motions, fluorescence studies via the covalent incorporation of conformation-sensitive dyes have the unique advantage to allow for the investigation of receptors in purified but also cell-expressed environment. Voltage-clamp fluorometry (VCF), which probes simultaneously fluorescent changes and electrophysiological currents in real time, has been particularly successful in providing insights onto the dynamics of conformational changes at intermediate states that are silent in electrophysiology. Labeling of the muscle nAChR (αγαδβ subtype) at the top of TMD (position 19′ located at the upper end of M2 and facing the ECD) reported a conformational change of a monoliganded receptor that does not involve channel opening and occurs with fast kinetics (131). A somewhat similar phenotype was described for the α4β4 receptor in the extracellular loop 5 that faces the vestibule, suggesting that Ach and the competitive antagonist dihydro-beta-erythroidine elicits allosterically movements of this region without activation (132). A related phenotype was observed and investigated in depth on GLIC (133) and α1-GlyR (134). In addition, VCF of α1-GlyR labelled at the ECD-TMD interface showed that the receptor transits through a cluster of intermediate states characterized by robust fluorescence variations but no currents (134). These intermediates are stabilized in different pharmacological conditions, including low Gly concentrations, saturating concentrations of the partial agonist taurine and β-alanine, and mixtures of the competitive antagonist strychnine and glycine. By

[1] *Weak coupling* here stands for statistical rather than mechanical coupling, which is typically referred to as strong coupling in the field of molecular motors.

contrast, the general anesthetic propofol that binds to the TMD, destabilizes them favoring the isomerization to the active conformation in the presence of agonist. MD simulations further showed that this atypical pharmacological profile is compatible with the contribution of cluster of conformations derived from a taurine-bound closed structure solved by cryo-EM (112), that are characterized by a high flexibility of the ECD and the orthosteric site. With GLIC, a "pre-activation" phenotype was reported for a series of fluorescent sensors at the ECD and the M2-M3 loop at the ECD-TMD interface (133). In this case, pre-activation concerns mainly a quaternary compaction of the ECD that precedes the reorganization of a ECD-TMD interface involving contraction of the extracellular β-sandwiches and tilting of the pore-lining helices M2 (122). Altogether, fluorescence data point to an unanticipated structural plasticity of nAChRs and homologs that populate a dynamic intermediate state on the way to activation featuring a marked asymmetric organization of the protein. These intermediate conformations, exacerbated in loss-of-function mutants, may contribute to the transition pathways as dead-ends precluding channel opening or transient states preceding activation.

A second family of "late" gating intermediates was inferred from kinetic analyses of single-channel recordings. Measurement of close-to-open transition kinetics and fitting using multistate models suggest that channel activation at GlyR and muscle nAChR both involve a transient population of short-lived intermediate states named "flipped" (135) and "primed" (136). Of note, the allosteric equilibrium between flipped and active appears to be independent of the nature of the ligand bound at the orthosteric site, thus suggesting it is a late intermediate where the ECD has completed activation.

Overall, functional data by VCF and single-channel electrophysiology are consistent with a progressive propagation of the gating transition from the orthosteric site to the ion pore in the form of a *conformational wave*. The emerging mechanism involves distinct clusters of "early" (by VCF) and "late" (by single-channel electrophysiology) intermediate conformations that are silent in electrophysiology but contribute to the channel activation path (**Figure 3B**), thereby impacting the time course of the gating currents. Importantly, these intermediates underly the distinct action of agonists, antagonists, and partial agonists and are likely relevant for drug discovery. We note that single-channel recordings of mutants of the muscle nAChR analyzed by REFERs (rate equilibrium linear free energy relationships) are consistent with an early motion of the ECD, especially of the orthosteric site and the M2-M3 loop, and a late motion of the TMD during channel activation (137).

4.4 Towards a general mechanism of signal transduction

The combination of high-resolution structures, *in silico* simulations, voltage-clamp fluorometry, and single-channel recordings highlights common traits of the molecular mechanism(s) of signal transduction by nAChRs and receptor homologs. The long-range allosteric communication between the orthosteric site and the ion channel gate, which are distant >50 Å within the protein structure, does not imply an all-or-none concerted reorganization but rather a progressive conformational wave. The agonists stabilize a local perturbation at the orthosteric site that propagates from the ECD to the TMD. Along this path, the receptor visits several metastable intermediate conformations, especially when the propagating signal "encounters" the hinge at the ECD-TMD interface. Consistent with the MWC model, channel activation involves major quaternary reorganizations of the protein domains between discrete pre-existing states, which are stabilized by ligand-binding events and communicated at the ECD-TMD interface via shape complementarity. The subunit interfaces as well as the ECD-TMD interface thus play a key role in signal propagation, starting from the C-loop and F-loop at the orthosteric sites, to the M2-M3 loop that is directly connected to the pore-lining helix M2. The emerging mechanism of activation appears to be conserved virtually in all pLGICs from bacteria to human, with important consequences in the mode of action of allosteric effectors. By contrast, the mechanism of desensitization requires further investigation and current models based on anionic pLGICs might not apply to nAChRs.

5. Implications for Drug Discovery

Beside the illumination of the conformational changes underlying activation and desensitization, the various atomic structures of nAChRs provide 3D templates of the orthosteric site and several allosteric modulatory sites that can be used for drug design. In addition, it has been shown that in the limit of the MWC model, quantitative predictions of the pharmacological attributes of potency, efficacy and selectivity of the modulatory ligands can be obtained from the ligand-binding affinities for the resting, the active and the desensitized states of the receptor (138); see **Figure 4**. This offers a general theoretical framework for allosteric drug design, which we termed *state-based* or *conformation-specific pharmacology* (138). Because ligand-binding affinities for discrete conformational states of nAChRs are difficult to measure experimentally, this framework for drug design is best suited for simulation analyses and binding free energy calculations.

Since the first high-resolution structures of AChBP, modeling approached based on all-atom MD simulations have been implemented to obtain reliable binding free-energy estimates for nicotinic ligands. Early docking studies with empirical free-energy rescoring showed that agonists and antagonists could be correctly classified based on calculated affinities for the open- and closed-state homology models of α4β2-nAChR (139). Simplified binding free-energy calculations based on the molecular mechanics Poisson-Boltzmann surface area (MM/PBSA) method were able to reproduce relative binding affinities for 16 known agonists and identify two novel α7-selective agonists (140). Using quantum mechanical calculations on a model of the muscle nAChR, Beck *et al* explored the selectivity of nicotinoid and neonicotinoid ligands in human versus insect rationalizing why nicotine has limited efficacy as an insecticide (141). The rational design of potent and selective antagonists derived from α-conotoxins was achieved by *in silico* mutational scanning coupled to MM/GBSA free energy calculations, yielding new RegIIA variants that were shown to be selective at α3β2-nAChR versus α3β4-nAChR (142). Affinity calculations based on free-energy perturbation (FEP) of three α-conotoxins targeting α3β2-nAChR than α3β4-nAChR were shown to reproduce relative binding affinities and potencies for a series of single-point toxins mutants and used to predict 52 α3β2-selective toxin mutations in quantitative agreement with experiments (143). Last, highly accurate binding affinity results were recently reported for nicotine in AChBP using "alchemical" FEP calculations (144). The excellent retrospective performances of rigorous binding free energy calculations at nAChRs makes the rational design of agonists and antagonists within reach. In this context, the growing number of nAChR structures unraveling unique conformational states of the receptor including intermediates are most appealing for the development of novel classes of modulatory ligands.

6. Conclusion: A novel Allosteric Landscape

The nAChR is the first neurotransmitter receptor isolated and biochemically identified as homo- and hetero-pentameric membrane protein with a rotational axis of symmetry perpendicular to the plane of the membrane. Each individual subunit can be subdivided into three structural domains with distinct functions, i.e., the synaptic domain, a transmembrane domain, and a cytoplasmic domain. Extensive early biochemical studies demonstrated that nAChR is a *bona fide* allosteric protein carrying multiple categories of topographically distinct, and conformationally linked, ligand-binding sites.

Thanks to the discovery of nAChR homologs in prokaryotes, the 3D atomic structure of the first ligand gated ion channels have been established and subsequently found very similar

to other members of the nAChR superfamily, including eukaryotic GluCl, $GABA_A$, Glycine, $5HT_3$ receptors and, of course, several oligomeric sub-types of nAChRs. These high-resolution studies led to the description at the atomic level of the distinct categories of functional sites carried by these receptors and their variability. They include: the orthosteric site(s) for the neurotransmitter and homologs; the ion channel sites for channel blockers; and multiple allosteric modulatory sites distributed all over the protein molecule and with little or no structural homology with the orthosteric sites (with ivermectin among other ligands). These structural findings reveal a surprising bacterial phylogenetic origin of our brain receptors, plausibly imposing bottom-up constraints on the modulation of higher brain functions.

The fast (ms) conformational change, or allosteric transition, mediating the activation of the ion channel by ACh or homologs was initially identified biochemically by fluorescence spectroscopy, offering the first structural evidence for signal transduction beyond electrophysiological methods. The structural changes mediating activation have since been resolved at the atomic level with nAChR and homologs using high-resolution X-ray and cryo-EM methods and molecular dynamics simulations together with careful assessments of pore opening at each ion-channel state. Globally the data fit with the MWC two-state model yet with additional important particularities. Furthermore, simulation studies and joint fluorescence and patch-clamp analyses of the dynamics of the transition between discrete resting and active conformations reveals a complex propagation of the conformational change involving a number of short-lived pre-active intermediates.

At variance with classical allosteric proteins, nAChRs and homologs spontaneously occur under multiple interconvertible conformations including slowly accessible (100ms-sec) desensitized states, with higher affinity for agonists and most often closed channels. Their structure at high resolution demonstrates striking differences with the resting and active conformations. The plausible role of desensitization in the regulation of synapse efficacy as well as the molecular mechanism underlying the transition from active to desensitized need to be further explored.

The recent results of joint molecular dynamics and structural data of nAChRs and homologs create a double paradigmatic change in our current understanding of the mode of action of pharmacological agents and drug design:

First, drug action can no longer be viewed as a competitive interaction taking place by steric hindrance at the level of a common, rigid, binding site (145, 146). “Allosteric modulatory sites” which do not show any structural analogy with the orthosteric sites efficiently regulate

signal transduction and serve as novel, highly efficient targets with possibly less side-effects than orthosteric ligands.

Second, the detailed structural and functional identification of the several conformational states of nAChR and homologs at the atomic level paves the way to a new "conformation-specific pharmacology" resulting in the deliberate design of agonists vs antagonists vs desensitizing agents. This is of major importance for the pharmacological therapeutics of abundant neuropsychiatric disorders driven by nAChR (and homologs) in the organism. These include, among others, cognitive enhancement, nicotine addiction, learning and memory, neuroinflammation, schizophrenia, epilepsy, and degenerative diseases like Alzheimer's and Parkinson's and finally aging.

These data and perspectives further illustrate the critical role played in the past decades by nAChR as a structural and functional model for neurotransmitter receptors with important consequences for drug design and the therapeutics of neuro-psychiatric deficits.

Acknowledgements

The work was supported by the HBP Specific Grant Agreement No. 945539 (Human Brain Project SGA3), ERC (Grant no. 788974, Dynacotine), the "Agence Nationale de la Recherche" (Grant ANR-18-CE11-0015), and the European Union's Horizon 2020 MSCA Program under grant agreement 956314 (ALLODD).

References

1. Changeux J-P, Kasai M, Lee C-Y. 1970. Use of a Snake Venom Toxin to Characterize the Cholinergic Receptor Protein. *Proc. Natl. Acad. Sci.* 67(3):1241–47
2. Changeux J-P. 2020. Discovery of the First Neurotransmitter Receptor: The Acetylcholine Nicotinic Receptor. *Biomolecules*. 10(4):547
3. Chang CC, Lee CY. 1966. Electrophysiological study of neuromuscular blocking action of cobra neurotoxin. *Br. J. Pharmacol. Chemother.* 28(2):172–81
4. Langley JN. 1905. On the reaction of cells and of nerve-endings to certain poisons, chiefly as regards the reaction of striated muscle to nicotine and to curari. *J. Physiol.* 33(4–5):374–413
5. Katz B, Thesleff S. 1957. A study of the 'desensitization' produced by acetylcholine at the motor end-plate. *J. Physiol.* 138(1):63–80
6. Sakmann B, Patlak J, Neher E. 1980. Single acetylcholine-activated channels show burst-kinetics in presence of desensitizing concentrations of agonist. *Nature*. 286(5768):71–73
7. Heidmann T, Changeux J-P. 1979. Fast Kinetic Studies on the Interaction of a Fluorescent Agonist with the Membrane-Bound Acetylcholine Receptor from Torpedo marmorata. *Eur. J. Biochem.* 94(1):255–79

8. Boyd ND, Cohen JB. 1980. Kinetics of binding of [3H]acetylcholine and [3H]carbamoylcholine to Torpedo postsynaptic membranes: slow conformational transitions of the cholinergic receptor. *Biochemistry*. 19(23):5344–53
9. Grünhagen H-H, Changeux J-P. 1976. Studies on the electrogenic action of acetylcholine with Torpedo marmorata electric organ. *J. Mol. Biol.* 106(3):497–516
10. Galzi JL, Revah F, Bessis A, Changeux JP. 1991. Functional Architecture of the Nicotinic Acetylcholine Receptor: From Electric Organ to Brain. *Annu. Rev. Pharmacol. Toxicol.* 31(1):37–72
11. Changeux J-P, Edelstein SJ. 2005. Allosteric Mechanisms of Signal Transduction. *Science*. 308(5727):1424–28
12. Heidmann T, Bernhardt J, Neumann E, Changeux JP. 1983. Rapid kinetics of agonist binding and permeability response analyzed in parallel on acetylcholine receptor rich membranes from Torpedo marmorata. *Biochemistry*. 22(23):5452–59
13. Dunn SMJ, Blanchard SG, Raftery MA. 1980. Kinetics of carbamylcholine binding to membrane-bound acetylcholine receptor monitored by fluorescence changes of a covalently bound probe. *Biochemistry*. 19(24):5645–52
14. Heidmann T, Changeux J-P. 1980. Interaction of a fluorescent agonist with the membrane-bound acetylcholine receptor from Torpedomarmorata in the millisecond time range: Resolution of an “intermediate” conformational transition and evidence for positive cooperative effects. *Biochem. Biophys. Res. Commun.* 97(3):889–96
15. Monod J, Wyman J, Changeux J-P. 1965. On the nature of allosteric transitions: A plausible model. *J. Mol. Biol.* 12(1):88–118
16. Katz B, Thesleff S. 1957. On the factors which determine the amplitude of the ‘miniature end-plate potential.’ *J. Physiol.* 137(2):267–78
17. Changeux J-P. 1990. The TiPS lecture the nicotinic acetylcholine receptor: an allosteric protein prototype of ligand-gated ion channels. *Trends Pharmacol. Sci.* 11(12):485–92
18. Nemecz Á, Prevost MS, Menny A, Corringer P-J. 2016. Emerging Molecular Mechanisms of Signal Transduction in Pentameric Ligand-Gated Ion Channels. *Neuron*. 90(3):452–70
19. Cecchini M, Changeux J-P. 2015. The nicotinic acetylcholine receptor and its prokaryotic homologues: Structure, conformational transitions & allosteric modulation. *Neuropharmacology*. 96:137–49
20. Jackson MB. 1986. Kinetics of unliganded acetylcholine receptor channel gating. *Biophys. J.* 49(3):663–72
21. Changeux J-P. 2018. The nicotinic acetylcholine receptor: a typical ‘allosteric machine.’ *Philos. Trans. R. Soc. B Biol. Sci.* 373(1749):20170174
22. Corringer P-J, Novère NL, Changeux J-P. 2000. Nicotinic Receptors at the Amino Acid Level. *Annu. Rev. Pharmacol. Toxicol.* 40(1):431–58
23. Zhong W, Gallivan JP, Zhang Y, Li L, Lester HA, Dougherty DA. 1998. From *ab initio* quantum mechanics to molecular neurobiology: A cation–π binding site in the nicotinic receptor. *Proc. Natl. Acad. Sci.* 95(21):12088–93
24. Neher E. 1983. The charge carried by single-channel currents of rat cultured muscle cells in the presence of local anaesthetics. *J. Physiol.* 339(1):663–78
25. Giraudat J, Dennis M, Heidmann T, Haumont PY, Lederer F, Changeux JP. 1987. Structure of the high-affinity binding site for noncompetitive blockers of the acetylcholine receptor: [3H]chlorpromazine labels homologous residues in the .beta. and .delta. chains. *Biochemistry*. 26(9):2410–18

26. Giraudat J, Dennis M, Heidmann T, Chang JY, Changeux JP. 1986. Structure of the high-affinity binding site for noncompetitive blockers of the acetylcholine receptor: serine-262 of the delta subunit is labeled by [3H]chlorpromazine. *Proc. Natl. Acad. Sci.* 83(8):2719–23
27. Hucho F, Oberthür W, Lottspeich F. 1986. The ion channel of the nicotinic acetylcholine receptor is formed by the homologous helices M II of the receptor subunits. *FEBS Lett.* 205(1):137–42
28. Corringer P-J, Baaden M, Bocquet N, Delarue M, Dufresne V, et al. 2010. Atomic structure and dynamics of pentameric ligand-gated ion channels: new insight from bacterial homologues: Pentameric ligand-gated ion channels. *J. Physiol.* 588(4):565–72
29. Imoto K, Busch C, Sakmann B, Mishina M, Konno T, et al. 1988. Rings of negatively charged amino acids determine the acetylcholine receptor channel conductance. *Nature*. 335(6191):645–48
30. Leonard RJ, Labarca CG, Charnet P, Davidson N, Lester HA. 1988. Evidence That the M2 Membrane-Spanning Region Lines the Ion Channel Pore of the Nicotinic Receptor. *Science*. 242(4885):1578–81
31. Corringer P-J, Bertrand S, Galzi J-L, Devillers-Thiéry A, Changeux J-P, Bertrand D. 1999. Mutational Analysis of the Charge Selectivity Filter of the α7 Nicotinic Acetylcholine Receptor. *Neuron*. 22(4):831–43
32. Möhler H, Okada T. 1977. Benzodiazepine Receptor: Demonstration in the Central Nervous System. *Science*. 198(4319):849–51
33. Sternbach LH. 1978. The benzodiazepine story. In *Progress in Drug Research / Fortschritte der Arzneimittelforschung / Progrès des recherches pharmaceutiques*, ed E Jucker, pp. 229–66. Basel: Birkhäuser Basel
34. Galzi J-L, Changeux J-P. 1994. Neurotransmitter-gated ion channels as unconventional allosteric proteins. *Curr. Opin. Struct. Biol.* 4(4):554–65
35. Olsen RW, Lindemeyer AK, Wallner M, Li X, Huynh KW, Zhou ZH. 2019. Cryo-electron microscopy reveals informative details of GABAA receptor structural pharmacology: implications for drug discovery. *Ann. Transl. Med.* 7(S3):S144–S144
36. Mulle C, Léna C, Changeux J-P. 1992. Potentiation of nicotinic receptor response by external calcium in rat central neurons. *Neuron*. 8(5):937–45
37. Vernino S, Amador M, Luetje CW, Patrick J, Dani JA. 1992. Calcium modulation and high calcium permeability of neuronal nicotinic acetylcholine receptors. *Neuron*. 8(1):127–34
38. Galzi JL, Bertrand S, Corringer PJ, Changeux JP, Bertrand D. 1996. Identification of calcium binding sites that regulate potentiation of a neuronal nicotinic acetylcholine receptor. *EMBO J.* 15(21):5824–32
39. Le Novère N, Grutter T, Changeux J-P. 2002. Models of the extracellular domain of the nicotinic receptors and of agonist- and Ca^{2+} -binding sites. *Proc. Natl. Acad. Sci.* 99(5):3210–15
40. Ananchenko A, Hussein TOK, Mody D, Thompson MJ, Baenziger JE. 2022. Recent Insight into Lipid Binding and Lipid Modulation of Pentameric Ligand-Gated Ion Channels. *Biomolecules*. 12(6):814
41. Barrantes FJ. 2023. Structure and function meet at the nicotinic acetylcholine receptor-lipid interface. *Pharmacol. Res.* 190:106729

42. Nury H, Van Renterghem C, Weng Y, Tran A, Baaden M, et al. 2011. X-ray structures of general anaesthetics bound to a pentameric ligand-gated ion channel. *Nature*. 469(7330):428–31
43. Campbell WC. 2016. Ivermectin: A Reflection on Simplicity (Nobel Lecture). *Angew. Chem. Int. Ed.* 55(35):10184–89
44. Krause RM, Buisson B, Bertrand S, Corringer P-J, Galzi J-L, et al. 1998. Ivermectin: A Positive Allosteric Effector of the α7 Neuronal Nicotinic Acetylcholine Receptor. *Mol. Pharmacol.* 53(2):283–94
45. Chen I-S, Kubo Y. 2018. Ivermectin and its target molecules: shared and unique modulation mechanisms of ion channels and receptors by ivermectin: Modulation mechanisms of ivermectin targets. *J. Physiol.* 596(10):1833–45
46. Papke RL, Lindstrom JM. 2020. Nicotinic acetylcholine receptors: Conventional and unconventional ligands and signaling. *Neuropharmacology*. 168:108021
47. Papke RL, Kem WR, Soti F, López-Hernández GY, Horenstein NA. 2009. Activation and desensitization of nicotinic alpha7-type acetylcholine receptors by benzylidene anabaseines and nicotine. *J. Pharmacol. Exp. Ther.* 329(2):791–807
48. Krause RM, Buisson B, Bertrand S, Corringer P-J, Galzi J-L, et al. 1998. Ivermectin: A Positive Allosteric Effector of the α7 Neuronal Nicotinic Acetylcholine Receptor. *Mol. Pharmacol.* 53(2):283–94
49. Zwart R, De Filippi G, Broad LM, McPhie GI, Pearson KH, et al. 2002. 5-Hydroxyindole potentiates human alpha 7 nicotinic receptor-mediated responses and enhances acetylcholine-induced glutamate release in cerebellar slices. *Neuropharmacology*. 43(3):374–84
50. Hurst RS, Hajós M, Raggenbass M, Wall TM, Higdon NR, et al. 2005. A Novel Positive Allosteric Modulator of the α7 Neuronal Nicotinic Acetylcholine Receptor: In Vitro and In Vivo Characterization. *J. Neurosci.* 25(17):4396–4405
51. Gill JK, Dhankher P, Sheppard TD, Sher E, Millar NS. 2012. A Series of α7 Nicotinic Acetylcholine Receptor Allosteric Modulators with Close Chemical Similarity but Diverse Pharmacological Properties. *Mol. Pharmacol.* 81(5):710–18
52. Cecchini M, Brando F, Changeux J-P. 2023. ACRALL – The Nicotinic Acetylcholine Receptor Allosteric Ligand Library (v1)
53. Swope SL, Qu Z, Huganir RL. 1995. Phosphorylation of the Nicotinic Acetylcholine Receptor by Protein Tyrosine Kinasesa. *Ann. N. Y. Acad. Sci.* 757(1):197–214
54. Lee Y, Rudell J, Yechikhov S, Taylor R, Swope S, Ferns M. 2008. Rapsyn carboxyl terminal domains mediate muscle specific kinase–induced phosphorylation of the muscle acetylcholine receptor. *Neuroscience*. 153(4):997–1007
55. Liao X, Wang Y, Lai X, Wang S. 2023. The role of Rapsyn in neuromuscular junction and congenital myasthenic syndrome. *Biomol. Biomed.*
56. Kabbani N, Nichols RA. 2018. Beyond the Channel: Metabotropic Signaling by Nicotinic Receptors. *Trends Pharmacol. Sci.* 39(4):354–66
57. Kabbani N, Woll MP, Levenson R, Lindstrom JM, Changeux J-P. 2007. Intracellular complexes of the β2 subunit of the nicotinic acetylcholine receptor in brain identified by proteomics. *Proc. Natl. Acad. Sci.* 104(51):20570–75
58. Cartaud J, Popot J-L, Changeux J-P. 1980. Light and heavy forms of the acetylcholine receptor from *Torpedo marmorata* electric organ: Morphological identification using reconstituted vesicles. *FEBS Lett.* 121(2):327–32

59. Cartaud J, Benedetti EL, Cohen JB, Meunier J-C, Changeux J-P. 1973. Presence of a lattice structure in membrane fragments rich in nicotinic receptor protein from the electric organ of *Torpedo marmorata*. *FEBS Lett.* 33(1):109–13
60. Klymkowsky MW, Stroud RM. 1979. Immunospecific identification and three-dimensional structure of a membrane-bound acetylcholine receptor from Torpedo californica. *J. Mol. Biol.* 128(3):319–34
61. Brisson A, Unwin PNT. 1985. Quaternary structure of the acetylcholine receptor. *Nature*. 315(6019):474–77
62. Miyazawa A, Fujiyoshi Y, Stowell M, Unwin N. 1999. Nicotinic acetylcholine receptor at 4.6 Å resolution: transverse tunnels in the channel 1 1Edited by J. Karn. *J. Mol. Biol.* 288(4):765–86
63. Brejc K, Van Dijk WJ, Klaassen RV, Schuurmans M, Van Der Oost J, et al. 2001. Crystal structure of an ACh-binding protein reveals the ligand-binding domain of nicotinic receptors. *Nature*. 411(6835):269–76
64. Tasneem A, Iyer LM, Jakobsson E, Aravind L. 2004. Identification of the prokaryotic ligand-gated ion channels and their implications for the mechanisms and origins of animal Cys-loop ion channels. *Genome Biol.* 6(1):R4
65. Bocquet N, Prado De Carvalho L, Cartaud J, Neyton J, Le Poupon C, et al. 2007. A prokaryotic proton-gated ion channel from the nicotinic acetylcholine receptor family. *Nature*. 445(7123):116–19
66. Hilf RJC, Dutzler R. 2008. X-ray structure of a prokaryotic pentameric ligand-gated ion channel. *Nature*. 452(7185):375–79
67. Bocquet N, Nury H, Baaden M, Le Poupon C, Changeux J-P, et al. 2009. X-ray structure of a pentameric ligand-gated ion channel in an apparently open conformation. *Nature*. 457(7225):111–14
68. Prevost MS, Sauguet L, Nury H, Van Renterghem C, Huon C, et al. 2012. A locally closed conformation of a bacterial pentameric proton-gated ion channel. *Nat. Struct. Mol. Biol.* 19(6):642–49
69. Sauguet L, Shahsavar A, Poitevin F, Huon C, Menny A, et al. 2014. Crystal structures of a pentameric ligand-gated ion channel provide a mechanism for activation. *Proc. Natl. Acad. Sci.* 111(3):966–71
70. Hu H, Nemecz Á, Van Renterghem C, Fourati Z, Sauguet L, et al. 2018. Crystal structures of a pentameric ion channel gated by alkaline pH show a widely open pore and identify a cavity for modulation. *Proc. Natl. Acad. Sci.* 115(17):
71. Hu H, Howard RJ, Bastolla U, Lindahl E, Delarue M. 2020. Structural basis for allosteric transitions of a multidomain pentameric ligand-gated ion channel. *Proc. Natl. Acad. Sci.* 117(24):13437–46
72. Hibbs RE, Gouaux E. 2011. Principles of activation and permeation in an anion-selective Cys-loop receptor. *Nature*. 474(7349):54–60
73. Du J, Lü W, Wu S, Cheng Y, Gouaux E. 2015. Glycine receptor mechanism elucidated by electron cryo-microscopy. *Nature*. 526(7572):224–29
74. Miller PS, Aricescu AR. 2014. Crystal structure of a human GABAA receptor. *Nature*. 512(7514):270–75
75. Hassaine G, Deluz C, Grasso L, Wyss R, Tol MB, et al. 2014. X-ray structure of the mouse serotonin 5-HT3 receptor. *Nature*. 512(7514):276–81
76. Morales-Perez CL, Noviello CM, Hibbs RE. 2016. X-ray structure of the human α4β2 nicotinic receptor. *Nature*. 538(7625):411–15

77. Gharpure A, Noviello CM, Hibbs RE. 2020. Progress in nicotinic receptor structural biology. *Neuropharmacology*. 171:108086
78. Langenbuch-Cachat J, Bon C, Mulle C, Goeldner M, Hirth C, Changeux JP. 1988. Photoaffinity labeling of the acetylcholine binding sites on the nicotinic receptor by an aryldiazonium derivative. *Biochemistry*. 27(7):2337–45
79. Dennis M, Giraudat J, Kotzyba-Hibert F, Goeldner M, Hirth C, et al. 1988. Amino acids of the Torpedo marmorata acetylcholine receptor .alpha. subunit labeled by a photoaffinity ligand for the acetylcholine binding site. *Biochemistry*. 27(7):2346–57
80. Giraudat J, Dennis M, Heidmann T, Changeux JP, Bisson R, et al. 1986. Tertiary Structure of the Nicotinic Acetylcholine Receptor Probed by Photolabeling and Protein Chemistry. In *Nicotinic Acetylcholine Receptor*, ed A Maelicke, pp. 103–14. Berlin, Heidelberg: Springer Berlin Heidelberg
81. Gharpure A, Teng J, Zhuang Y, Noviello CM, Walsh RM, et al. 2019. Agonist Selectivity and Ion Permeation in the α3β4 Ganglionic Nicotinic Receptor. *Neuron*. 104(3):501-511.e6
82. Rahman MdM, Teng J, Worrell BT, Noviello CM, Lee M, et al. 2020. Structure of the Native Muscle-type Nicotinic Receptor and Inhibition by Snake Venom Toxins. *Neuron*. 106(6):952-962.e5
83. Nys M, Zarkadas E, Brams M, Mehregan A, Kambara K, et al. 2022. The molecular mechanism of snake short-chain α-neurotoxin binding to muscle-type nicotinic acetylcholine receptors. *Nat. Commun.* 13(1):4543
84. Noviello CM, Gharpure A, Mukhtasimova N, Cabuco R, Baxter L, et al. 2021. Structure and gating mechanism of the α7 nicotinic acetylcholine receptor. *Cell*. 184(8):2121-2134.e13
85. Rahman MdM, Basta T, Teng J, Lee M, Worrell BT, et al. 2022. Structural mechanism of muscle nicotinic receptor desensitization and block by curare. *Nat. Struct. Mol. Biol.* 29(4):386–94
86. Goswami U, Rahman MM, Teng J, Hibbs RE. 2023. Structural interplay of anesthetics and paralytics on muscle nicotinic receptors. *Nat. Commun.* 14(1):3169
87. Zhao Y, Liu S, Zhou Y, Zhang M, Chen H, et al. 2021. Structural basis of human α7 nicotinic acetylcholine receptor activation. *Cell Res.* 31(6):713–16
88. Zarkadas E, Pebay-Peyroula E, Thompson MJ, Schoehn G, Uchański T, et al. 2022. Conformational transitions and ligand-binding to a muscle-type nicotinic acetylcholine receptor. *Neuron*. 110(8):1358-1370.e5
89. Bertrand S, Devillers-Thiéry A, Palma E, Buisson B, Edelstein SJ, et al. 1997. Paradoxical allosteric effects of competitive inhibitors on neuronal α7 nicotinic receptor mutants: *NeuroReport*. 8(16):3591–96
90. Revah F, Bertrand D, Galzi J-L, Devillers-Thiéry A, Mulle C, et al. 1991. Mutations in the channel domain alter desensitization of a neuronal nicotinic receptor. *Nature*. 353(6347):846–49
91. Smart OS, Neduvelil JG, Wang X, Wallace BA, Sansom MSP. 1996. HOLE: A program for the analysis of the pore dimensions of ion channel structural models. *J. Mol. Graph.* 14(6):354–60
92. Klesse G, Rao S, Sansom MSP, Tucker SJ. 2019. CHAP: A Versatile Tool for the Structural and Functional Annotation of Ion Channel Pores. *J. Mol. Biol.* 431(17):3353–65
93. Beckstein O, Sansom MSP. 2006. A hydrophobic gate in an ion channel: the closed state of the nicotinic acetylcholine receptor. *Phys. Biol.* 3(2):147–59

94. Gielen M, Thomas P, Smart TG. 2015. The desensitization gate of inhibitory Cys-loop receptors. *Nat. Commun.* 6(1):6829
95. Zhuang Y, Noviello CM, Hibbs RE, Howard RJ, Lindahl E. 2022. Differential interactions of resting, activated, and desensitized states of the α7 nicotinic acetylcholine receptor with lipidic modulators. *Proc. Natl. Acad. Sci.* 119(43):e2208081119
96. Polovinkin L, Hassaine G, Perot J, Neumann E, Jensen AA, et al. 2018. Conformational transitions of the serotonin 5-HT3 receptor. *Nature*. 563(7730):275–79
97. Changeux J-P. *Functional architecture and dynamics of the Nicotinic Acetylcholine Receptor: an Allosteric Ligand-Gated Ion Channel. Fidia Research Foundation Neuroscience Award Lectures*. Raven press New-York
98. Bondarenko V, Wells MM, Chen Q, Tillman TS, Singewald K, et al. 2022. Structures of highly flexible intracellular domain of human α7 nicotinic acetylcholine receptor. *Nat. Commun.* 13(1):793
99. Huang X, Chen H, Shaffer PL. 2017. Crystal Structures of Human GlyRα3 Bound to Ivermectin. *Structure*. 25(6):945-950.e2
100. Bondarenko V, Chen Q, Singewald K, Haloi N, Tillman TS, et al. 2023. Structural Elucidation of Ivermectin Binding to α7nAChR and the Induced Channel Desensitization. *ACS Chem. Neurosci.* 14(6):1156–65
101. Prevost MS, Barilone N, Dejean De La Batie G, Pons S, Ayme G, et al. 2023. An original potentiating mechanism revealed by the cryoEM structures of the human α7 nicotinic receptor in complex with nanobodies. Neuroscience
102. Zimmermann I, Dutzler R. 2011. Ligand Activation of the Prokaryotic Pentameric Ligand-Gated Ion Channel ELIC. *PLoS Biol.* 9(6):e1001101
103. Li Q, Nemecz Á, Aymé G, Dejean De La Bâtie G, Prevost MS, et al. 2023. Generation of nanobodies acting as silent and positive allosteric modulators of the α7 nicotinic acetylcholine receptor. *Cell. Mol. Life Sci.* 80(6):164
104. Zhu S, Noviello CM, Teng J, Walsh RM, Kim JJ, Hibbs RE. 2018. Structure of a human synaptic GABAA receptor. *Nature*. 559(7712):67–72
105. Olsen RW. 2018. GABAA receptor: Positive and negative allosteric modulators. *Neuropharmacology*. 136:10–22
106. Huang X, Shaffer PL, Ayube S, Bregman H, Chen H, et al. 2017. Crystal structures of human glycine receptor α3 bound to a novel class of analgesic potentiators. *Nat. Struct. Mol. Biol.* 24(2):108–13
107. Delbart F, Brams M, Gruss F, Noppen S, Peigneur S, et al. 2018. An allosteric binding site of the α7 nicotinic acetylcholine receptor revealed in a humanized acetylcholine-binding protein. *J. Biol. Chem.* 293(7):2534–45
108. Laha KT, Ghosh B, Czajkowski C. 2013. Macroscopic Kinetics of Pentameric Ligand Gated Ion Channels: Comparisons between Two Prokaryotic Channels and One Eukaryotic Channel. *PLoS ONE*. 8(11):e80322
109. Trick JL, Chelvaniththilan S, Klesse G, Aryal P, Wallace EJ, et al. 2016. Functional Annotation of Ion Channel Structures by Molecular Simulation. *Structure*. 24(12):2207–16
110. Cerdan AH, Martin NÉ, Cecchini M. 2018. An Ion-Permeable State of the Glycine Receptor Captured by Molecular Dynamics. *Structure*. 26(11):1555-1562.e4
111. Cerdan AH, Cecchini M. 2020. On the Functional Annotation of Open-Channel Structures in the Glycine Receptor. *Structure*. 28(6):690-693.e3

112. Yu J, Zhu H, Lape R, Greiner T, Du J, et al. 2021. Mechanism of gating and partial agonist action in the glycine receptor. *Cell*. 184(4):957-968.e21
113. Cerdan AH, Peverini L, Changeux J-P, Corringer P-J, Cecchini M. 2022. Lateral fenestrations in the extracellular domain of the glycine receptor contribute to the main chloride permeation pathway. *Sci. Adv.* 8(41):eadc9340
114. Law RJ, Henchman RH, McCammon JA. 2005. A gating mechanism proposed from a simulation of a human α7 nicotinic acetylcholine receptor. *Proc. Natl. Acad. Sci.* 102(19):6813–18
115. Cheng X, Wang H, Grant B, Sine SM, McCammon JA. 2006. Targeted Molecular Dynamics Study of C-Loop Closure and Channel Gating in Nicotinic Receptors. *PLoS Comput. Biol.* 2(9):e134
116. Nury H, Poitevin F, Van Renterghem C, Changeux J-P, Corringer P-J, et al. 2010. One-microsecond molecular dynamics simulation of channel gating in a nicotinic receptor homologue. *Proc. Natl. Acad. Sci.* 107(14):6275–80
117. Martin NE, Malik S, Calimet N, Changeux J-P, Cecchini M. 2017. Un-gating and allosteric modulation of a pentameric ligand-gated ion channel captured by molecular dynamics. *PLOS Comput. Biol.* 13(10):e1005784
118. Calimet N, Simoes M, Changeux J-P, Karplus M, Taly A, Cecchini M. 2013. A gating mechanism of pentameric ligand-gated ion channels. *Proc. Natl. Acad. Sci.* 110(42):
119. Althoff T, Hibbs RE, Banerjee S, Gouaux E. 2014. X-ray structures of GluCl in apo states reveal a gating mechanism of Cys-loop receptors. *Nature*. 512(7514):333–37
120. Yuan S, Filipek S, Vogel H. 2016. A Gating Mechanism of the Serotonin 5-HT 3 Receptor. *Structure*. 24(5):816–25
121. Lev B, Murail S, Poitevin F, Cromer BA, Baaden M, et al. 2017. String method solution of the gating pathways for a pentameric ligand-gated ion channel. *Proc. Natl. Acad. Sci.* 114(21):
122. Lefebvre SN, Taly A, Menny A, Medjebeur K, Corringer P-J. 2021. Mutational analysis to explore long-range allosteric couplings involved in a pentameric channel receptor pre-activation and activation. *eLife*. 10:e60682
123. Oliveira ASF, Shoemark DK, Campello HR, Wonnacott S, Gallagher T, et al. 2019. Identification of the Initial Steps in Signal Transduction in the α4β2 Nicotinic Receptor: Insights from Equilibrium and Nonequilibrium Simulations. *Structure*. 27(7):1171-1183.e3
124. Oliveira ASF, Edsall CJ, Woods CJ, Bates P, Nunez GV, et al. 2019. A General Mechanism for Signal Propagation in the Nicotinic Acetylcholine Receptor Family. *J. Am. Chem. Soc.* 141(51):19953–58
125. Bondarenko V, Mowrey DD, Tillman TS, Seyoum E, Xu Y, Tang P. 2014. NMR structures of the human α7 nAChR transmembrane domain and associated anesthetic binding sites. *Biochim. Biophys. Acta BBA - Biomembr.* 1838(5):1389–95
126. Nury H, Bocquet N, Le Poupon C, Raynal B, Haouz A, et al. 2010. Crystal Structure of the Extracellular Domain of a Bacterial Ligand-Gated Ion Channel. *J. Mol. Biol.* 395(5):1114–27
127. Duret G, Van Renterghem C, Weng Y, Prevost M, Moraga-Cid G, et al. 2011. Functional prokaryotic–eukaryotic chimera from the pentameric ligand-gated ion channel family. *Proc. Natl. Acad. Sci.* 108(29):12143–48

128. Cymes GD, Grosman C. 2021. Signal transduction through Cys-loop receptors is mediated by the nonspecific bumping of closely apposed domains. *Proc. Natl. Acad. Sci.* 118(14):e2021016118
129. Blanc F, Isabet T, Benisty H, Sweeney HL, Cecchini M, Houdusse A. 2018. An intermediate along the recovery stroke of myosin VI revealed by X-ray crystallography and molecular dynamics. *Proc. Natl. Acad. Sci.* 115(24):6213–18
130. Blanc FE, Cecchini M. 2021. An Asymmetric Mechanism in a Symmetric Molecular Machine. *J. Phys. Chem. Lett.* 12(13):3260–65
131. Dahan DS, Dibas MI, Petersson EJ, Auyeung VC, Chanda B, et al. 2004. A fluorophore attached to nicotinic acetylcholine receptor βM2 detects productive binding of agonist to the αδ site. *Proc. Natl. Acad. Sci.* 101(27):10195–200
132. Mourot A, Bamberg E, Rettinger J. 2008. Agonist- and competitive antagonist-induced movement of loop 5 on the α subunit of the neuronal α4β4 nicotinic acetylcholine receptor. *J. Neurochem.* 105(2):413–24
133. Menny A, Lefebvre SN, Schmidpeter PA, Drège E, Fourati Z, et al. 2017. Identification of a pre-active conformation of a pentameric channel receptor. *eLife*. 6:e23955
134. Shi S, Lefebvre SN, Peverini L, Cerdan AH, Milán Rodríguez P, et al. 2023. Illumination of a progressive allosteric mechanism mediating the glycine receptor activation. *Nat. Commun.* 14(1):795
135. Lape R, Colquhoun D, Sivilotti LG. 2008. On the nature of partial agonism in the nicotinic receptor superfamily. *Nature*. 454(7205):722–27
136. Mukhtasimova N, Lee WY, Wang H-L, Sine SM. 2009. Detection and trapping of intermediate states priming nicotinic receptor channel opening. *Nature*. 459(7245):451–54
137. Gupta S, Chakraborty S, Vij R, Auerbach A. 2017. A mechanism for acetylcholine receptor gating based on structure, coupling, phi, and flip. *J. Gen. Physiol.* 149(1):85–103
138. Cecchini M, Changeux J-P. 2022. Nicotinic receptors: From protein allostery to computational neuropharmacology. *Mol. Aspects Med.* 84:101044
139. Huang X, Zheng F, Zhan C-G. 2008. Modeling Differential Binding of α4β2 Nicotinic Acetylcholine Receptor with Agonists and Antagonists. *J. Am. Chem. Soc.* 130(49):16691–96
140. Grazioso G, Pomè DY, Matera C, Frigerio F, Pucci L, et al. 2009. Design of novel α7-subtype-preferring nicotinic acetylcholine receptor agonists: Application of docking and MM-PBSA computational approaches, synthetic and pharmacological studies. *Bioorg. Med. Chem. Lett.* 19(22):6353–57
141. Beck ME, Riplinger C, Neese F, Bistoni G. 2021. Unraveling individual HOST–GUEST interactions in molecular recognition from first principles quantum mechanics: Insights into the nature of nicotinic acetylcholine receptor agonist binding. *J. Comput. Chem.* 42(5):293–302
142. Xu Q, Tae H-S, Wang Z, Jiang T, Adams DJ, Yu R. 2020. Rational Design of α-Conotoxin RegIIA Analogues Selectively Inhibiting the Human α3β2 Nicotinic Acetylcholine Receptor through Computational Scanning. *ACS Chem. Neurosci.* 11(18):2804–11
143. Katz D, DiMattia MA, Sindhikara D, Li H, Abraham N, Leffler AE. 2021. Potency- and Selectivity-Enhancing Mutations of Conotoxins for Nicotinic Acetylcholine Receptors Can Be Predicted Using Accurate Free-Energy Calculations. *Mar. Drugs*. 19(7):367

144. Li Z, Chan KC, Nickels JD, Cheng X. 2022. Electrostatic Contributions to the Binding Free Energy of Nicotine to the Acetylcholine Binding Protein. *J. Phys. Chem. B*. 126(43):8669–79
145. Bovet D. 1957. The relationships between isosterism and competitive phenomena in the field of drug therapy of the autonomic nervous system and that of the neuromuscular transmission. *Proc Nobel Lect.*, pp. 552–78
146. Black J. 1989. Drugs from emasculated hormones: The principle of syntopic antagonism. *In Vitro Cell. Dev. Biol.* 25(4):311–20

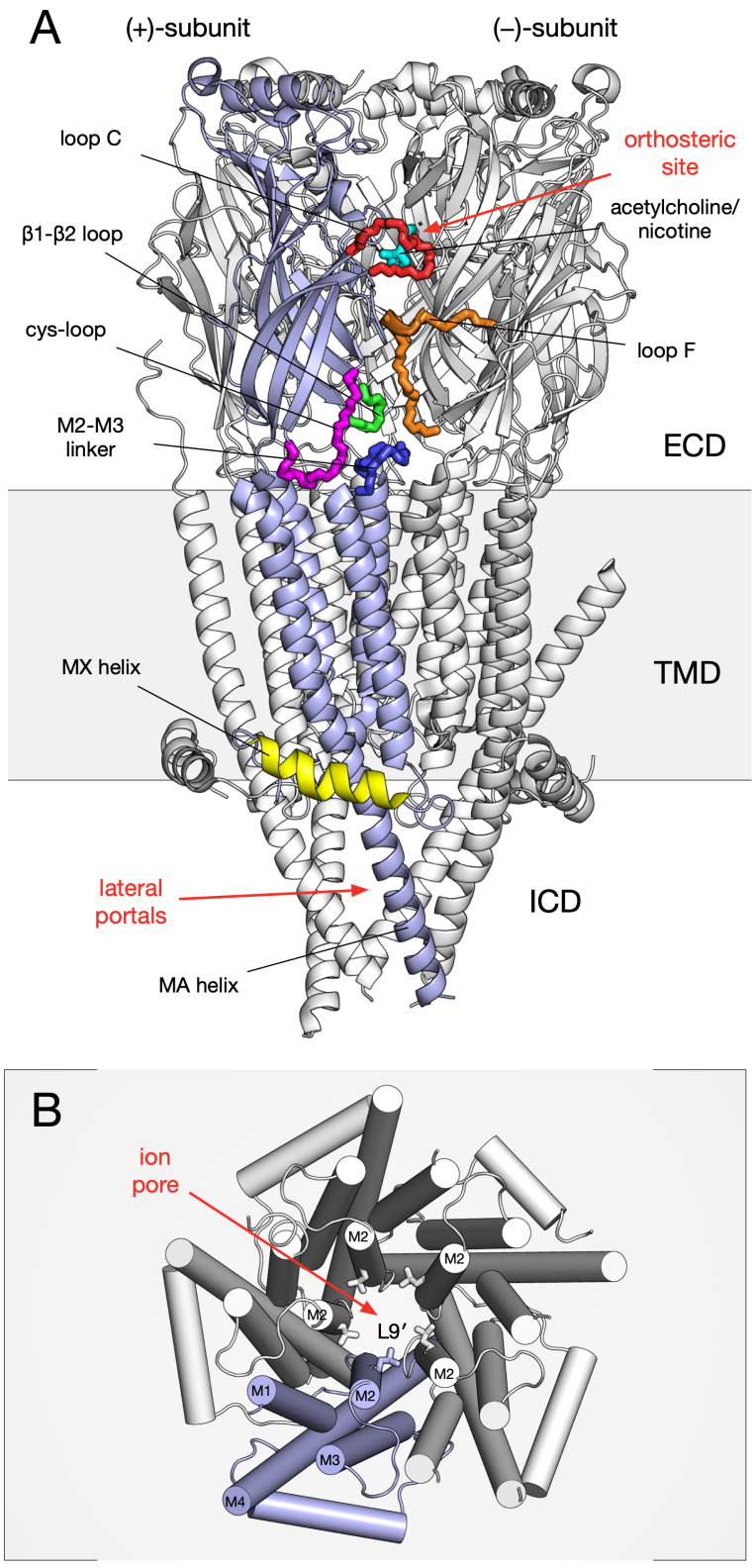

Figure 1. Molecular architecture of the nAChR. *For illustration, the high-resolution structure of the muscle-type nAChR solved in complex with nicotine (PDB: 7QL5) is shown. The protein is shown in cartoons, the lipid membrane as a grey box. One of the two α-subunits is highlighted in light blue. The structural features discussed in the Main Text are highlighted in bright colors. (A) Side view. The extracellular domain (ECD), the transmembrane domain (TMD), and the intracellular domain (ICD) of the receptor are visualized. (B) Top view. The pentameric organization and the structure of the TMD are shown. The five leucine residues on the pore-lining helices M2 at the activation gate (i.e., Leu 9′) are shown in sticks.*

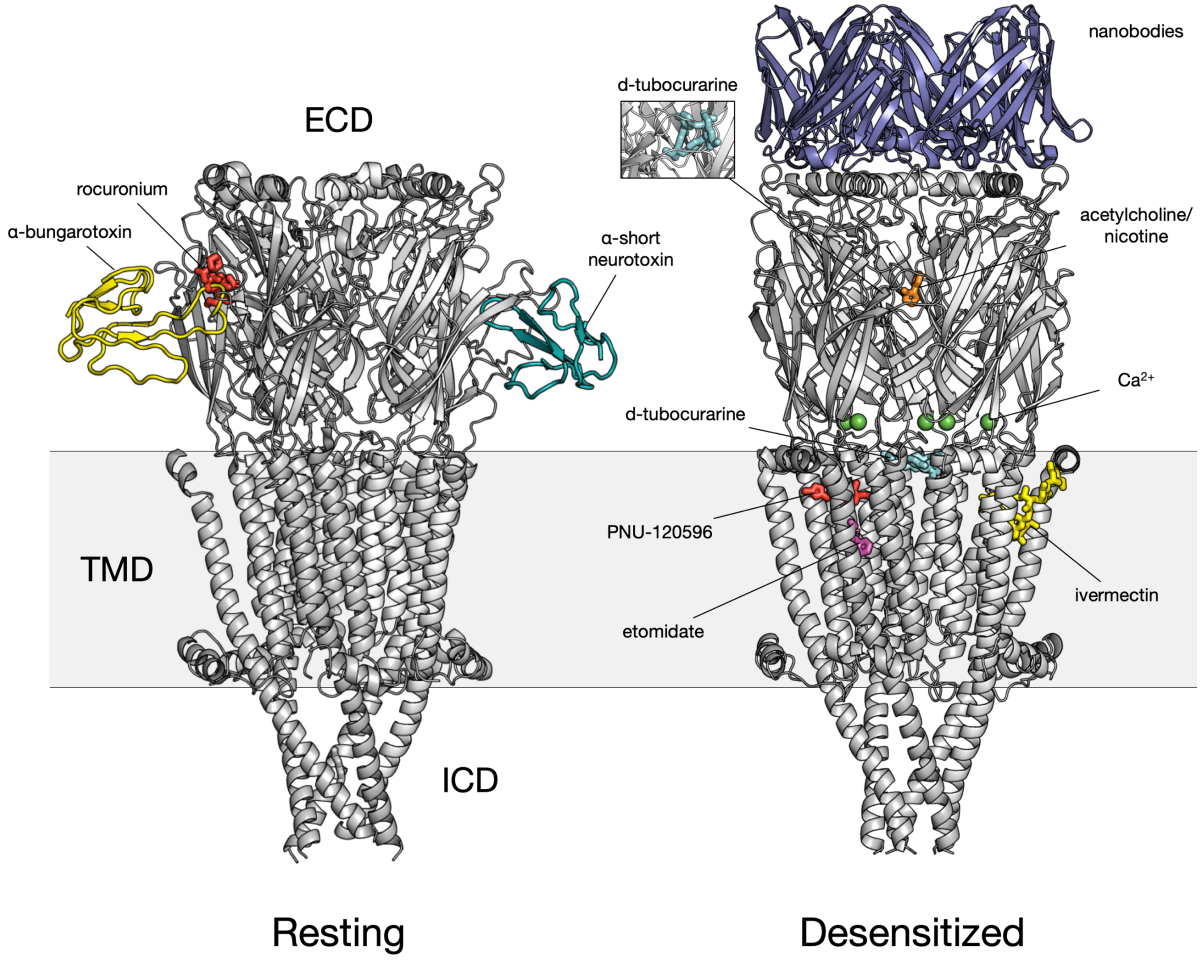

Figure 2. The orthosteric and allosteric ligand-binding sites at nAChR illuminated by high-resolution structures of intact receptors. *On the left-hand side, the structure of the muscle nAChR in complex with α-bungarotoxin (PDB: 6UWZ) is shown. On the right-hand side, the structure of α7-AChR solved in complex with EVP-6124 and the type-II positive allosteric modulator PNU-120596 (PDB:7EKT) is shown. These structures are representative of the resting and desensitized states of nAChRs, respectively. Coordinates of the modulatory compounds (in colors) were extracted from corresponding high-resolution structures upon superimposition to reference structures for resting and desensitized. As discussed in the Main Text, competitive antagonists like snake toxins and neuromuscular blockers (e.g., rocuronium) bind to the ECD in the resting state. Agonists (e.g., acetylcholine/nicotine), competitive antagonists enhancing desensitization (e.g., d-tubocurarine), PAMs targeting the ECD (e.g., nanobodies), the TMD (e.g., PNU or ivermectin) or the ECD-TMD interface (e.g., calcium ions), and NAMs (e.g., etomidate) bind preferentially to the active or the desensitized state.*

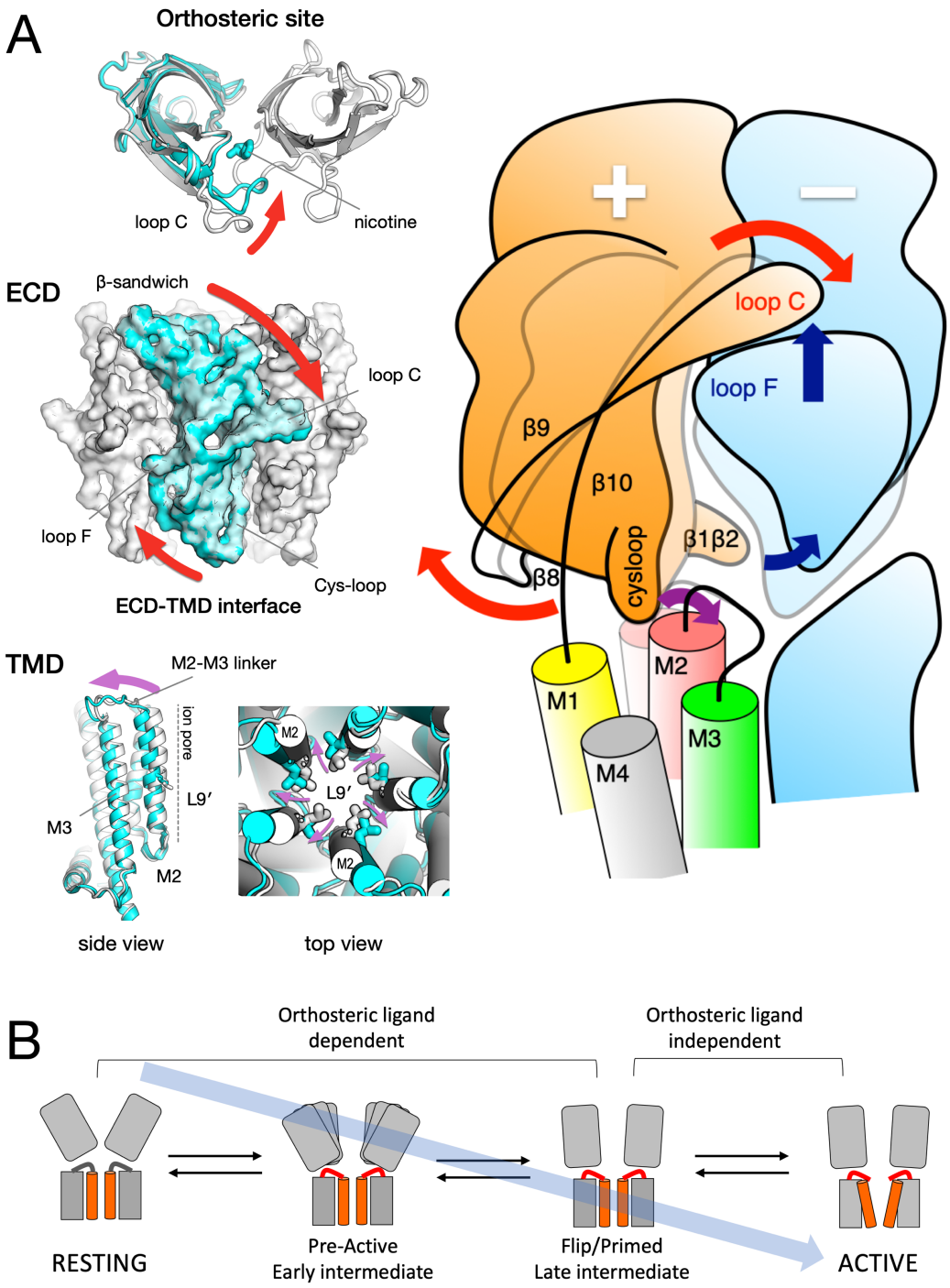

Figure 3: The molecular mechanism of nAChR activation. *(A) The conformational wave of gating as derived from high-resolution structures and simulation studies. The sequence of structural events translating agonist binding into pore opening is shown from top to bottom. On the left, the structures of the muscle nAChR apo (PDB: 7QKO, white) and in complex with nicotine (PDB: 7QL5, cyan) are shown to illustrate the conformational changes mediating channel activation. On the right, the cartoon representation of the conformational wave was adapted from Zarkadas et al (88). Agonist binding (i.e., nicotine) to the ECD elicits a significant contraction of the orthosteric site characterized by a large displacement of the C-loop that "closes" over it. Closing of C-loop coupled to the global tilting of the extracellular β-sandwiches promotes the repositioning of several loops including β1β2, β8β9, and the Cys-loop, thus transmitting the signal to the ECD-TMD interface. These rearrangements facilitate the translation of the M2-M3 linker in the outward direction, which occurs with significant tilting of the pore-lining helices M2. The resulting expansion of the ion pore along with rotameric transitions of bulky and hydrophobic residues that open the activation gate (i.e., L9') promote pore wetting and ion permeation. (B) The progressive mechanism of activation of nAChRs highlighting intermediate conformations deduced from combined fluorescence and electrophysiological observations (pre-active) and from kinetic analysis of single-channel recordings (Flip/primed). nAChRs are simplified as dimers, with the channel-lining helix M2 as orange cylinders, and the permeant cations as green spheres.*

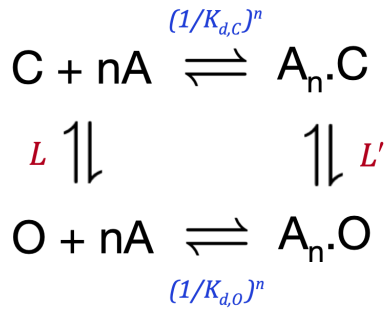

Potency

$$EC_{50} = \frac{K_{d,O}}{\sqrt{L}}$$

Efficacy

$$P_o^{\max} = \frac{L\left(\frac{K_{d,C}}{K_{d,O}}\right)^n}{1 + L\left(\frac{K_{d,C}}{K_{d,O}}\right)^n}$$

Selectivity

$$K_{\alpha,\beta} = \frac{K_{d,O}(\alpha)}{K_{d,O}(\beta)}\sqrt{\frac{L_\beta}{L_\alpha}}$$

Figure 4. Pharmacological attributes of the modulatory ligands as predicted by the MWC model. *Assuming that the open (O) and closed (C) states of the ion channel preexist in reversible equilibrium both in presence and absence of agonist (A), the model predicts agonist potency (EC_{50}), efficacy (P_o^{max}), and binding selectivity for α versus β can be predicted from the ligand-binding affinities for the open (1/Kd,O) and closed (1/Kd,C) states of the receptor (138). The equations shown that the pharmacological attributes depend on the unliganded gating constant (L) and the number of agonists bound (n).*